Chinese Chemical Letters 33 (2022) 1353–1357

Contents lists available at ScienceDirect

Chinese Chemical Letters

journal homepage: www.elsevier.com/locate/cclet

A new Eu-MOF for ratiometrically fluorescent detection toward quinolone antibiotics and selective detection toward tetracycline antibiotics

Chao-Yang Wang[a], Chong-Chen Wang[a,*], Xiu-Wu Zhang[a], Xue-Ying Ren[a], Baoyi Yu[b], Peng Wang[a], Zi-Xuan Zhao[a], Huifen Fu[a]

[a] Beijing Key Laboratory of Functional Materials for Building Structure and Environment Remediation/Beijing Energy Conservation & Sustainable Urban and Rural Development Provincial and Ministry Co-construction Collaboration Innovation Center, Beijing University of Civil Engineering and Architecture, Beijing 100044, China

[b] Key Laboratory of Urban Agriculture (North China), Ministry of Agriculture, College of Biological Sciences Engineering, Beijing University of Agriculture, Beijing 102206, China

ARTICLE INFO

Article history:
Received 27 June 2021
Revised 12 August 2021
Accepted 20 August 2021
Available online 27 August 2021

Keywords:
Metal-organic framework
Fluorescent detection
Sensor
Quinolone antibiotics
Tetracyclines antibiotics

ABSTRACT

Development of new self-calibrating fluorescent sensing methods has been a popular research field with the aim of protecting the human health and environment sustainability. In this work, a novel Eu-based metal organic framework (MOF) Eu(2,6-NDC)(COO) (**BUC-88**) was developed by employing 2,6-NDC (2,6-naphthalenedicarboxylic acid) as bridging ligands. **BUC-88** performed different sensing process toward quinolone antibiotics and tetracyclines antibiotics in terms of fluorescence intensity and color. **BUC-88** exhibited excellent selectivity and sensitivity detection property toward enrofloxacin (ENR), norfloxacin (NOR) and ciprofloxacin (CIP) over other Pharmaceutical and Personal Care Products (PPCPs), accomplishing the detection limit of 0.12 μmol/L, 0.52 μmol/L, 0.75 μmol/L, respectively. Notably, **BUC-88** acted as an excellent fluorescence sensor for tetracyclines antibiotics with fast response time (less than 1 s), high selectivity and sensitivity (LODs = 0.08 μmol/L). The fluorescent detection method was successfully used for visual and ultrasensitive detection of ENR, NOR, CIP and tetracycline hydrochloride (TC) in lake water with satisfied recovery from 99.75% to 102.30%. Finally, the photoinduced electron transfer and the competitive absorption of ultraviolet light are the main mechanisms for sensitive detection toward quinolone antibiotics and tetracyclines antibiotics.

Quinolone antibiotics and tetracyclines antibiotics as broad-spectrum antibiotics showed excellent curative effect on infections caused by various Gram-positive and negative bacteria [1]. These residual antibiotics still kept their biological activity, and could cause seriously environmental problems, such as aquatic organisms and terrestrial animals destruction and bacterial resistance increases [2-4]. Therefore, the selective and convenient recognition of quinolone antibiotics and tetracyclines antibiotics is critical tasks for protecting the environment sustainability and human health [5,6]. Currently, various techniques have been explored to detect these trace PPCPs pollutants, such as gas chromatography-mass spectrometry (GC-MS), liquid chromatography-mass spectrometry (LC-MS), electrochemical sensors and biosensors [7-9]. However, the above-stated methods are operationally complicated, time-consuming and high-cost, which severely limits real-time and field monitoring of PPCPs in the environment [7]. Fluorescent sensing technology is attracting increasing attention in past few decades due to their low cost, high sensitivity, short reaction time and good selectivity [10,11].

Metal-organic frameworks (MOFs) are a class of porous crystalline materials constructed by metal nodes and organic ligands through self-assembly [12,13]. Compared with the traditional transition metal elements MOFs, lanthanide MOFs (Ln-MOFs) possess some merits like larger Storks shift, higher quantum yields and longer lifetime [7,10,14-16], which made them promising fluorescent sensors for detecting environmental pollutants. In previous reports, the researchers mainly focused on using fluorescent MOFs to detect explosives, heavy-metal ions, viruses and so on [17]. Recently, fabrication of new fluorescent MOFs for sensing toward trace antibiotics has become a research hotspot [7,17]. In this work, a new 3D Ln-MOF Eu(2,6-NDC)(COO) (**BUC-88**, **BUC** refers to the

* Corresponding author.
E-mail address: chongchenwang@126.com (C.-C. Wang).

https://doi.org/10.1016/j.cclet.2021.08.095
1001-8417/

abbreviation of Beijing University of Civil Engineering and Architecture, the number **88** is the serial number of the new MOF synthesized by our group) was developed to accomplish ratiometrically fluorescent sensing toward quinolone antibiotics and selective detection toward tetracycline antibiotics. In addition, the fluorescent film of **BUC-88** was prepared from nail polish for sensing detection of quinolone and tetracycline antibiotics in water. In addition, the **BUC-88** fluorescent film has been successfully prepared with nail polish to achieve sensing detect toward quinolones and tetracycline antibiotics in water. The possible mechanisms for fluorescent responses toward quinolone antibiotics and tetracycline antibiotics were also discussed and tested.

Single crystal X-ray diffraction analysis (Table S1 in Supporting information) revealed that **BUC-88** crystallizes in the monoclinic crystal system of the $P2_1/c$ space group. The asymmetric structural unit of 3D **BUC-88** consists of one Eu^{3+}ion, four completely deprotonated 2,6-NDC anions (NDC^{2-}) ligands, and three deprotonated formic acid ligands (Fig. S1 in Supporting information). The Eu^{3+} ions were eight-coordinated by four oxygen atoms from four 2,6-NDC ligands and four oxygen atoms from two formic acid ligands to construct a distorted square antiprism EuO_8, in which the Eu-O distances were in the range of 2.287(6)–2.610(4) Å (Table S2 in Supporting information). The deprotonated NDC^{2-} anions are connected to four Eu^{3+} ions as a bidentate bridging linker between two adjacent inorganic ribbons, with the μ_4-η_1:η_1:η_1:η_1 conformation (syn-syn and syn-anti bidentate modes) [18], which form natural 2D metal-organic layer containing the advent of binuclear building blocks in the (*b, c*) plane. It is interesting to observe that formic acid ligands were derived from the in-situ decomposition of N,N-dimethylformamide (DMF) in the hydrothermal reaction process [18,19]. The 3D structure of **BUC-88** was formed by the NDC^{2-} ligands through connecting the organic-inorganic layers along the *a*-axis.

The experimental powder X-ray diffraction (PXRD) patterns of **BUC-88** (Figs. S2-S4 in Supporting information) matched well with the simulated one, indicating high water stability of **BUC-88**. The Fourier-transform infrared (FTIR) spectrum (Fig. S5 in Supporting information) analysis and thermal investigations and stability analysis (Figs. S6 and S7 in Supporting information) were described in the supporting information.

The quantum yield and fluorescent lifetime of **BUC-88** were 29.27% and 0.592 ms (Fig. S8 in Supporting information), respectively, which indicated the good energy migration from ligand triplet state to lanthanide receiving energy level [20]. Comparing to the UV–vis DRS spectra of 2,6-NDC, the absorption bands of **BUC-88** were slightly red-shifted in the range of 230–300 nm, which could be attributed to the deprotonation of 2,6-NDC and the coordination with Eu^{3+} ions (Fig. S9 in Supporting information) [21]. The solid-state excitation and emission spectra of the 2,6-NDC ligand showed a broad emission peak at 400–460 nm with the maximum peak at 421 nm (Fig. 1a), which could be assigned to the ligand-based π^*-π and/or π^*-n transitions of the 2,6-NDC ligand [22,23].

Commission Internationale d'Éclairage (CIE) chromaticity diagram of 2,6-NDC ligand (0.1540, 0.0628) and **BUC-88** (0.6264, 0.3241) were displayed in the Figs. 1b and d, further confirming that 2,6-NDC ligand and **BUC-88** exhibited the blue and light red at excitation wavelength of 387 nm [24]. The fluorescence spectra of solid **BUC-88** exhibited the characteristic emission peaks of Eu^{3+} ions except for the ligand emission spectra, implying the "antenna effect" taken place in **BUC-88** (Fig. 1c) [24]. Tight eight characteristic emission peaks at 579, 588, 594, 613, 616, 621, 654, and 700 nm were assigned to the $^5D_0 \rightarrow {}^7F_0$, $^5D_0 \rightarrow {}^7F_1$, $^5D_0 \rightarrow {}^7F_2$, $^5D_0 \rightarrow {}^7F_3$ and $^5D_0 \rightarrow {}^7F_4$ transitions, respectively [17,25]. $^5D_0 \rightarrow {}^7F_0$ transition is forbidden transition, but it could obtain intensity on account of the crystal field potential with low symmetry. The

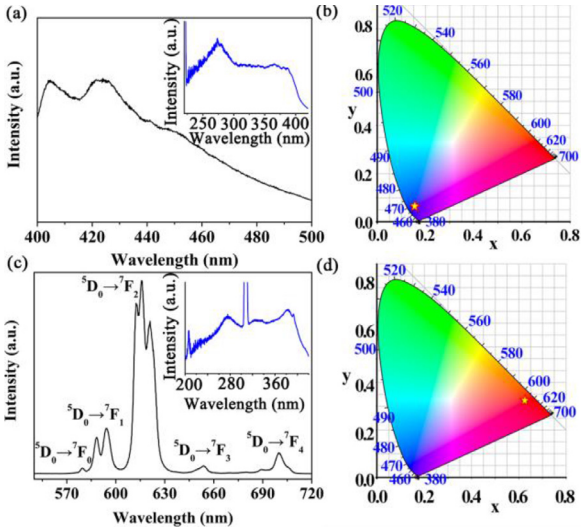

Fig. 1. (a) The fluorescence emission spectra of solid 2,6-NDC (inset: the excitation spectra of solid 2,6-NDC at the emission wavelength of 421 nm); (b) CIE chromaticity diagram showing the emissions of solid 2,6-NDC; (c) The fluorescence emission spectra of solid **BUC-88** (inset: the excitation spectra of solid **BUC-88** at the emission wavelength of 616 nm); (d) CIE chromaticity diagram showing the emissions of solid **BUC-88**.

$^5D_0 \rightarrow {}^7F_1$ transition is a magnetic dipole transition, and its intensity is changed with the crystal field around Eu^{3+}. What is more, the $^5D_0 \rightarrow {}^7F_2$ transition is an electric dipole transition, which is sensitive to chemical bonds in the vicinity of Eu^{3+} [24]. The intensity of the $^5D_0 \rightarrow {}^7F_2$ transition is about 4.2 times stronger than that of the $^5D_0 \rightarrow {}^7F_1$ transition, indicating the coordination environment of the europium cation is asymmetric [24,26]. The $^5D_0 \rightarrow {}^7F_3$ transition is an electric-dipole transition, which is depended on the site symmetry. The $^5D_0 \rightarrow {}^7F_4$ transition could be assigned to the forced electric dipole (FED) and dynamic coupling (DC).

The fluorescent properties of **BUC-88** in different pH were further measured. As illustrated in Fig. S10, **BUC-88** performed excellent fluorescent stability in the pH range of 4.0-10.0, indicating that **BUC-88** was a potential fluorescent sensor in water. As shown in Fig. S10 (Supporting information), the fluorescence intensity of **BUC-88** only fluctuated slightly with the immersing time increases, implying that **BUC-88** possesses high fluorescent stability in the sensing experiment. Inspired by the fascinating fluorescence and stability of **BUC-88** in water, it is possible to design a fluorescent sensor for sensing PPCPs. As shown in Figs. S11 and S12 (Supporting information), **BUC-88** demonstrated higher emission intensity at 439 nm and lower emission intensity at 615 nm in the aqueous solutions of ENR, NOR and CIP (10^{-4} mol/L). In addition, **BUC-88** exhibited no influence on the fluorescence intensity in the other PPCPs solutions. The results indicated that both the fluorescence sensitizing effect and fluorescence quenching effect appeared simultaneously in the quinolone antibiotics (ENR, NOR and CIP) [7], which made it possible to construct a ratiometric sensor for detection toward quinolone antibiotics. To further understand the selectivity of **BUC-88** toward quinolone antibiotics among various PPCPs, the relative fluorescence intensity ($I_{439\ nm}/I_{615\ nm}$) of **BUC-88** toward different PPCPs were record in Fig. S12. It was observed that the intensity of $I_{439\ nm}/I_{615\ nm}$ was controlled by the quinolone antibiotics, indicating that **BUC-88** was a selective and ratiometric sensor for quinolone antibiotics [10].

To explore the detection limit (LODs) of **BUC-88** toward ENR, NOR and CIP, 4 mg **BUC-88** powder was immersed in different concentrations of quinolone antibiotics solution (0-20 μmol/L). As

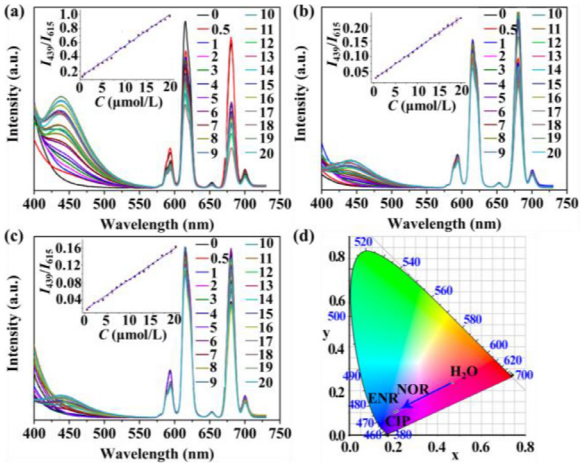

Fig. 2. Emission spectra and intensities of **BUC-88** dispersed in a series of concentration solution of (a) ENR, (b) NOR, (c) CIP (inset: the fluorescence intensities of **BUC-88** at 615 nm, E_x = 340 nm), (d) CIE chromaticity diagram showing the emissions of **BUC-88** in deionized water and quinolone antibiotics solution (10^{-4} mol/L).

shown in Figs. 2a-c, the fluorescence emission intensities of **BUC-88** at 615 nm were gradually decayed, while the emission intensities at 439 nm were instantly enhanced. The results further confirmed **BUC-88** was a ratiometric sensor for sensing quinolone antibiotics. The calibration curve based on $I_{439\ nm}/I_{615\ nm}$ versus quinolone antibiotics concentration ranging from 1.0 μmol/L to 20.0 μmol/L could be well expressed by the linear equation (Figs. 2a-c). Furthermore, the fluorescence changing degree, the ratiometric response efficiency, can be quantitatively explained using the Stern-Volmer (Eq. 1) [10]:

$$\frac{I_{439\ nm}}{I_{615\ nm}} = K_{SV}[Q] + 1 \quad (1)$$

where $I_{439\ nm}$ and $I_{615\ nm}$ are the fluorescent intensities of **BUC-88** at 439 nm and 615 nm in the presence of the analyte, respectively, [Q] is the molar concentration of the analyte, and K_{sv} is the quenching constant (L/mol).

Considering the excellent sensing properties of **BUC-88** toward quinolone antibiotics, the detection performance of **BUC-88** toward tetracyclines antibiotics were also studied. As shown in Figs. 2a-c, a good linear relationship between $I_{439\ nm}/I_{615\ nm}$ and the concentration quinolone antibiotics (ENR, NOR and CIP) were observed, with a correlation coefficient (R^2) of 0.9964, 0.9938, 0.9927, respectively. The K_{SV} values were calculated to be 4.41 × 10^4 L/mol (ENR), 1.03 × 10^4 L/mol (NOR) and 0.72 × 10^4 L/mol (CIP), which were higher than those of most reported in literatures (Table S3 in Supporting information) [7,24]. The LODs of **BUC-88** were valuated as low as 0.12 μmol/L (ENR), 0.53 μmol/L (NOR), 0.75 μmol/L (CIP) by using $3\sigma/S$ (σ = 0.0018, standard deviation of the fluorescent test for 20 blank solutions; S = slope of the calibration curve) [10]. The sensitivity of **BUC-88** for the detection of quinolone antibiotics is higher than those of the reported MOFs for the sensing of relevant antibiotics (Table S3). As illustrated in Fig. 2d, the CIE chromaticity diagrams of H_2O (0.4651, 0.2369), ENR (0.2037, 0.1023), NOR (0.2162, 0.1089) and CIP (0.2106, 0.1084) were further confirmed that the fluorescent color change process of **BUC-88** were induced by the quinolone antibiotics (10^{-4} mol/L).

The detection performance of **BUC-88** toward tetracyclines antibiotics were also studied. As shown in Figs. S13a and b (Supporting information), only the addition of tetracycline hydrochloride (TC), aureomycin (AM) or oxytetracycline (OTC) into the suspension of **BUC-88** could cause the significant fluorescence quenching, indicating **BUC-88** is a selective fluorescent sensor for tetracyclines

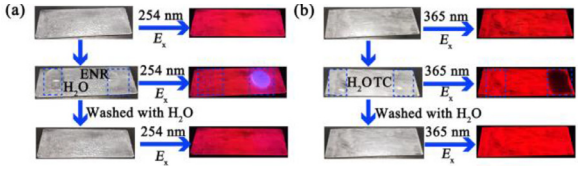

Fig. 3. **BUC-88** fluorescent sensing film is used for sensing (a) ENR and (b) TC.

antibiotics [7,10]. The anti-interference abilities of the tetracyclines antibiotics were evaluated by the response of fluorescence intensities of the **BUC-88** when TC was coexisting with other 14 PPCPs. The results showed that the fluorescence of **BUC-88** was quenched only with the presence of TC, further confirming **BUC-88** is a selective fluorescent sensor for TC [7,10]. In order to investigate the ions interference of **BUC-88** in response to TC, a wide range of relevant interfering species including metal ions (M = Na^+, K^+, Mg^{2+}, Ca^{2+}, Ba^{2+}, Cr^{3+}, Mn^{2+}, Co^{2+}, Ni^{2+}, Cu^{2+}, Ag^+, Zn^{2+}, Cd^{2+}, Al^{3+}, Fe^{2+}, Pb^{2+}, 10^{-3} mol/L for each) were studied by recording the fluorescence response of **BUC-88**. It is observed that **BUC-88** presented negligible fluorescence quenching effect toward selected co-existing metal ions (Figs. S13c and d in Supporting information), while exhibited significant quenching effect in the presence of TC in the system. The results indicated that **BUC-88** is a selective sensor for TC in water [10].

To obtain the LODs of TC, 4 mg **BUC-88** powder was immersed in a serious different concentration solution of TC (0.1μmol/L - 20 μmol/L). As expected, the fluorescence emissions intensities at 615 nm were instantly decayed as the concentration increases (less than 1 s), indicating that it is a fast and sensitive sensor to probe TC. As shown in Fig. S14 (Supporting information), the calibration curve based on I_0/I_{615nm} versus TC concentration ranging from 0.1 μmol/L to 10 μmol/L was illustrated, which could be well expressed by the linear equation of I_0/I_{615nm} = 0.1937 × [Q] (μmol/L) + 1.0043 with a correlation coefficient (R^2) of 0.9918. The sensitive response efficiency could be quantitatively explained using the Stern-Volmer in Eq. 2.

$$\frac{I_0}{I_{615nm}} = K_{SV}\ [Q] + 1 \quad (2)$$

where, I_0 and $I_{615\ nm}$ are the fluorescence intensities of **BUC-88** at 615 nm in the absence and presence of the analyte, respectively, [Q] is the molar concentration of the analyte, and K_{SV} is the quenching constant (L/mol). As shown in Fig. S14, a good linear relationship between analytical signal of $I_0/I_{615\ nm}$ and TC concentration is observed. The K_{SV} value was calculated to be 1.94 × 10^5 L/mol, which was higher to reported works that sensing of antibiotics in aqueous solutions (Table S3). The LODs was valuated as low as 0.08 μmol/L toward TC by using $3\sigma/S$ (σ = 0.0049, standard deviation of the fluorescence test for 20 blank solutions; S = slope of the calibration curve) [27], which was lower than those in most of the previous reports (Table S3). The sensitivity of **BUC-88** for the detection of tetracycline is superior to those of the reported MOFs for the sensing of relevant antibiotics (Table S3).

The reusability is one of the most important issues to evaluate the practical application value of fluorescent sensing materials [28]. **BUC-88** performed significant fluorescent changes in the aqueous solutions of ENR, NOR, CIP and TC, and the **BUC-88** could be easily regenerated by washing with deionized water for five times (Fig. 3a, Figs. S15 and S16 in Supporting information). The recyclable experiments revealed that **BUC-88** could act as an excellent fluorescent sensor for quinolone antibiotics and tetracyclines antibiotics [7].

To explore the possibility of practical application of **BUC-88**, the sensing properties for quinolone antibiotics and tetracyclines antibiotics in lake water samples were carried out. A standard addi-

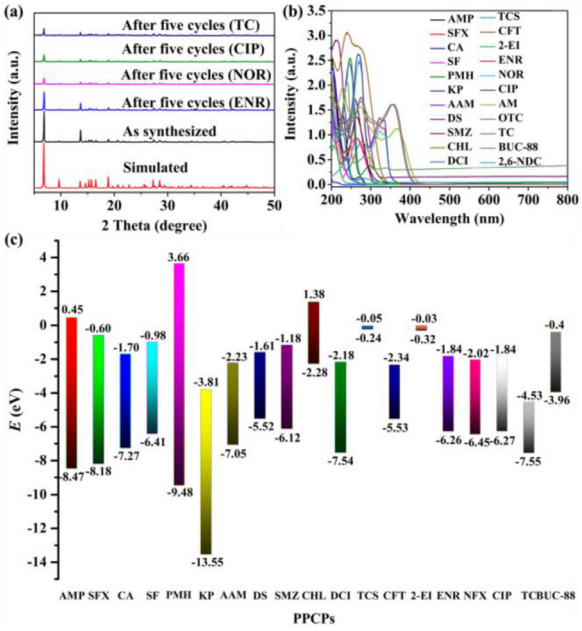

Fig. 4. (a) The PXRD patterns of **BUC-88** before and after the five cycles test; (b) UV–vis spectra of different PPCPs; (c) the calculated energy levels for the 2,6-NDC ligand and PPCPs molecules.

tion method was used to analyze the detection of ENR, NOR, CIP and TC in lake water samples. The results were shown in Table S4 (Supporting information), the recoveries of ENR, NOR, CIP and TC in lake water samples were between 99.51% and 103.15%. The relative standard deviations (RSD, $n = 3$) are all less than 0.83%. The results indicated that the detection of quinolone antibiotics and tetracyclines antibiotics by using **BUC-88** as fluorescent sensor showed good recovery and precision [7,29].

To further explore the practical application capability, fluorescent sensing film of **BUC-88** was prepared using a clear nail polish. As shown in Figs. 3a and b, the fluorescent color of the **BUC-88** film changed from red to blue when the quinolone antibiotics (10^{-3} mol/L) was dropped onto the slide, while the fluorescence was quenched completely when the tetracyclines antibiotics (10^{-3} mol/L) was drop onto the slide. Furthermore, when the film was cleaned with deionized water, the fluorescence returned to the original state. The PXRD patterns of **BUC-88** fluorescent film after immersing in deionized water for 10 days were identical to the as-synthesized one (Fig. S17 in Supporting information), indicating that **BUC-88** fluorescent film was highly stable in water. The results showed that **BUC-88** has a strong practical application prospect in sensing quinolone antibiotics and tetracyclines antibiotics.

The structure collapse, electrons transfer, and energy distribution are significant factors for the fluorescent sensing behavior [17]. To investigate the fluorescent quenching mechanism, PXRD, FTIR, SEM of **BUC-88** before and after testing ENR, NOR, CIP and TC were recorded. The lifetime of **BUC-88** before and after sensing ENR, NOR, CIP and TC were shown in Figs. S18 and S19 (Supporting information). It is clear that the lifetime of **BUC-88** unchanged after the sensing tests, illustrating the static quenching was dominant in the sensing process [17]. As shown in Fig. 4a, the structure of **BUC-88** still maintained its integrity after the five cycles tests, which demonstrated that the fluorescence quenching is not due to the collapse of the framework [7,17]. The SEM of **BUC-88** further confirmed the structure integrity of **BUC-88** after the five cycles test (Fig. S20 in Supporting information). After the cycling experiments, no new stretching vibration peaks appeared in the FTIR spectra of the as-synthesized samples (Fig. S4), indicating that **BUC-88** had no chemical or physical adsorption effect on quinolone antibiotics and TC. To further establish the proposed mechanism for fluorescence quenching by quinolone antibiotics and tetracyclines antibiotics, detailed studies on the UV–vis absorption of different PPCPs were recorded (Fig. 4b). The absorption spectrum of quinolone antibiotics and tetracyclines antibiotics have large spectral overlaps with the excitation peaks of the ligand and **BUC-88** were observed, implying that the competitive energy absorption may be a possible reason for the fluorescent quenching [19]. Furthermore, it was proposed that the photoinduced electron transfer was a probable mechanism for the sensor's fluorescence quenching induced by the antibiotics [7,30]. In light of this, the energy levels of the ENR [7], NOR [7], CIP [7], AMP [31], SFX [32], CA [33], SF [34], PMH [35], KP [36], AAM [37], DS [38], SMZ [39], CHL [40], DCI [41], TCS [42], CFT [43], 2-EI [44], AM [10], OTC [10] and TC [45] were acquired (as calculated at the B3LYP/6–311G* level of theory). The flat-band potentials (E_{FB}) of **BUC-88** were recorded via typical Mott-Schottky measurements (Fig. S21 in Supporting information). The positive slope of C^2 values *versus* potential indicated **BUC-88** is a typical n-type semiconductors [46]. The E_{FB} of **BUC-88** determined from Mott-Schottky plots were *ca.* –0.6 eV *versus* the Ag/AgCl electrode. Therefore, the conduction band (CB) and lowest unoccupied molecular orbital (LUMO) of **BUC-88** is –0.4 eV. Obviously, quinolone antibiotics and tetracyclines antibiotics exhibited a lower LUMO energy level than that of the **BUC-88** (Fig. 4c), while the other PPCPs performed the similar LUMO energy level [7]. Hence, the high selectivity of **BUC-88** toward other PPCPs might be attribute to the lower LUMO level of quinolone antibiotics and tetracyclines antibiotics, and the excited electrons in **BUC-88** could be more easily transferred into quinolone antibiotics and tetracyclines antibiotics [30]. The results indicated that the photoinduced electron transfer was another possible reason for the fluorescence quenching [30]. However, the order of observed quenching efficiency was not completely accordance with the LUMO energy, indicating that photoinduced electron transfer was not the only mechanism for the fluorescence quenching. Above all, photo-competitive effect and photoinduced electron transfer were the mechanism for the fluorescence quenching of **BUC-88** in response to the quinolone antibiotics and tetracyclines antibiotics. In addition, ENR, NOR, and CIP had obvious adsorption peaks at 300–390 nm (Fig. S21), after adsorption, ENR, NOR, and CIP emitted blue light (Fig. S22 in Supporting information). The results also explain the fluorescence "turn-on" at 439 nm for ENR, NOR, and CIP.

In summary, a novel 3D porous red-light-emitting fluorescent sensor **BUC-88** has been successfully obtained. **BUC-88** presents as a water stable fluorescent Eu-MOF sensor to accomplish highly selective and sensitive detect toward quinolone antibiotics and tetracyclines antibiotics. Photophysical analysis revealed that **BUC-88** is an excellent bifunctional sensor, which could be used to sense quinolone antibiotics *via* a fluorescent color-changing process and detect tetracyclines antibiotics *via* a fluorescence quenching phenomenon. Additionally, the **BUC-88** as sensor could be simply and quickly regenerated, exhibiting excellent recyclability for the detection of quinolone antibiotics and tetracyclines antibiotics. Furthermore, the fluorescent **BUC-88** film was successfully developed for rapid and circular detection of quinolone antibiotics and tetracyclines antibiotics. This work demonstrated that fluorescent MOFs could be rationally designed and explored as potential fluorescent sensor and quantitative detection materials in environmental remediation areas.

Declaration of competing interest

The authors declare no conflict of interest.

Acknowledgements

This work was supported by National Natural Science Foundation of China (Nos. 51878023 and 21806008), Beijing Talent Project (No. 2020A27), The Fundamental Research Funds for Beijing University of Civil Engineering and Architecture (No. X20147/X20141/X20135/X20146).

Supplementary materials

Supplementary material associated with this article can be found, in the online version, at doi:10.1016/j.cclet.2021.08.095.

References

[1] S. Li, J. Hu, J. Hazard. Mater. 318 (2016) 134–144.
[2] R. Gothwal, T. Shashidhar, Clean-Soil Air Water 43 (2015) 479–489.
[3] A.G. Trovo, R.F.P. Nogueira, A. Agüera, et al., Water Res. 45 (2011) 1394–1402.
[4] S. Li, W. Shi, H. Li, et al., Sci. Total Environ. 636 (2018) 1009–1019.
[5] S. Li, J. Hu, Water Res. 132 (2018) 320–330.
[6] S. Li, T. Huang, P. Du, et al., Water Res. 185 (2020) 116286.
[7] W.B. Zhong, R.X. Li, J. Lv, Inorg. Chemi. Front. 7 (2020) 1161–1171.
[8] E. Benito-Peña, J. Urraca, M. Moreno-Bondi, J. Pharmaceut. Biomed. 49 (2009) 289–294.
[9] P. Jakubec, V. Urbanová, Z. Medříková, et al., Chem. Eur J. 22 (2016) 14279–14284.
[10] C. Li, W. Yang, X. Zhang, et al., J. Mater. Chem. C 8 (2020) 2054–2064.
[11] Y. Wan, Y. Cui, Y. Yang, et al., Chin. Chem. Lett. 32 (2021) 1511–1514.
[12] X.H. Yi, H. Ji, C.C. Wang, et al., Appl. Catal. B: Environ. 293 (2021) 120229.
[13] Y.C. Zhou, P. Wang, H. Fu, et al., Chin. Chem. Lett. 31 (2020) 2645–2650.
[14] Y. Li, X. Wang, C. Xing, et al., Chin. Chem. Lett. 30 (2019) 1440–1444.
[15] H. Wang, X. Wang, R.-.M. Kong, et al., Chin. Chem. Lett. 32 (2021) 198–202.
[16] K. Chen, C. Wu, Chin. Chem. Lett. 29 (2018) 823–826.
[17] W.P. Lustig, S. Mukherjee, N.D. Rudd, et al., Chem. Soc. Rev. 46 (2017) 3242–3285.
[18] I. Rodrigues, I. Mihalcea, C. Volkringer, et al., Inorg. Chem. 51 (2012) 483–490.
[19] G.C. Shearer, S. Chavan, S. Bordiga, et al., Chem. Mater. 28 (2016) 3749–3761.
[20] A.S. Borges, J.D.L. Dutra, R.O. Freire, et al., Inorg. Chem. 51 (2012) 12867–12878.
[21] C.Y. Wang, H. Fu, P. Wang, et al., Appl. Organomet. Chem. 33 (2019) e5021.
[22] M.D. Allendorf, C.A. Bauer, R. Bhakta, et al., Chem. Soc. Rev. 38 (2009) 1330–1352.
[23] X.Y. Guo, F. Zhao, J.J. Liu, et al., J. Mater. Chem. A 5 (2017) 20035–20043.
[24] M. Yu, Y. Xie, X. Wang, et al., ACS Appl. Mater. Interfaces 11 (2019) 21201–21210.
[25] Q.Y. Liu, W.F. Wang, Y.L. Wang, et al., Inorg. Chem. 51 (2012) 2381–2392.
[26] A.F. Kirby, F. Richardson, J. Phys. Chem. 87 (1983) 2544–2556.
[27] H. Xu, C.S. Cao, B. Zhao, Chem. Commun. 51 (2015) 10280–10283.
[28] W. Zhang, H. Huang, D. Liu, et al., Micropor. Mesopor. Mat. 171 (2013) 118–124.
[29] Y.Q. Zhang, X.H. Wu, S. Mao, et al., Talanta 204 (2019) 344–352.
[30] K. Zhu, R. Fan, X. Zheng, et al., J. Mater. Chem. C 7 (2019) 15057–15065.
[31] S.H. Kumar, S. Karthikeyan, J. Mater. Environ. Sci. 4 (2013) 675–984.
[32] S. Karthikeyan, P. Jeeva, Port. Electrochim. Act. 37 (2019) 307–315.
[33] M. Prabhaharan, A. Prabakaran, S. Srinivasan, et al., Spectrochim. Acta 138 (2015) 711–722.
[34] H.R. Obayes, A.A. Al-Amiery, G.H. Alwan, et al., J. Mol. Struct. 1138 (2017) 27–34.
[35] M.R. Ganjali, B. Vesimohammadi, S. Riahi, et al., Int. J. Electrochem. Sci. 4 (2009) 740–754.
[36] F. Kayadibi, S. Zor, S. Sagdinc, Prot. Met. Phys. Chem. 52 (2016) 356–371.
[37] D. Stummer, C. Herrmann, A. Rentmeister, ChemistryOpen 4 (2015) 295–301.
[38] J.R. de Andrade, M.F. Oliveira, R.L.S. Canevesi, et al., J. Mol. Liq. (2020) 113427.
[39] S. Luo, Z. Wei, R. Spinney, et al., J. Hazard. Mater. 343 (2018) 132–139.
[40] L. Xie, N. Xiao, L. Li, et al., Int. J. Mol. Sci. 21 (2020) 4139.
[41] A.M. Abuelela, M.A. Bedair, W.M. Zoghaib, et al., J. Mol. Struct. (2020) 129647.
[42] Y. Yue, Z. Wang, Y. Zhang, et al., Chemosphere 214 (2019) 278–287.
[43] X. Pang, M. Gong, Y. Zhang, et al., Sci. China Chem. 54 (2011) 1529–1536.
[44] M. Arivazhagan, S. Manivel, S. Jeyavijayan, et al., Spectrochim. Acta A 134 (2015) 493–501.
[45] A.H. Malik, P.K. Iyer, ACS Appl. Mater. Inter. 9 (2017) 4433–4439.
[46] V. Spagnol, E. Sutter, C. Debiemme-Chouvy, et al., Electrochim. Acta 54 (2009) 1228–1232.